



Chemical Potential Driven Reorganization of Anions between Stern and Diffuse Layers at the Air/Water Interface

J. Phys. Chem. C 2022, 126, 1140–1151

Present by Sam Sokhuoy

(Soft-matter optical spectroscopy, R1020, 2022/02/05)

Chemical Potential Driven Reorganization of Anions between Stern and Diffuse Layers at the Air/Water Interface

Raju R. Kumal, Srikanth Nayak, Wei Bu, and Ahmet Uysal*



Cite This: *J. Phys. Chem. C* 2022, 126, 1140–1151



Read Online

ACCESS |



Metrics & More

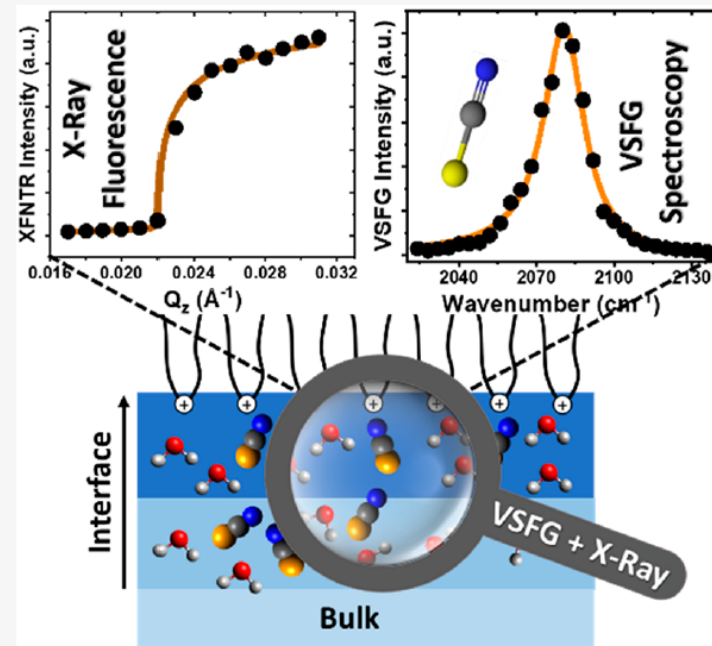


Article Recommendations



Supporting Information

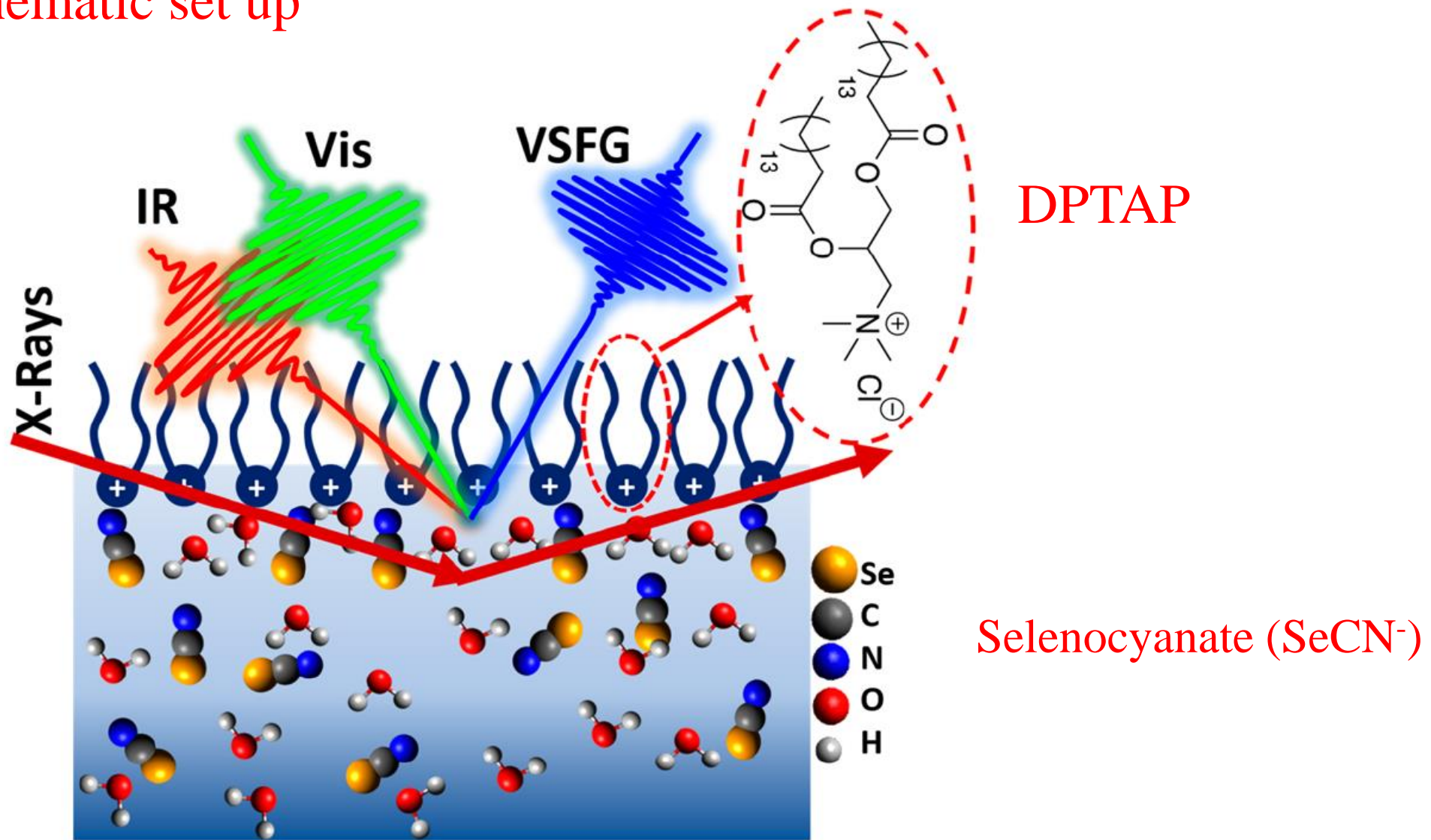
ABSTRACT: Ion adsorption and transfer at charged interfaces play key roles in various industrial and environmental processes. Molecular scale details of ion–ion, ion–water, and ion–surface interactions are still debated. Complex ions, such as SCN^- and SeCN^- , are particularly interesting due to their unexpected adsorption trends. Here, we combine vibrational sum frequency generation (VSFG) spectroscopy and surface-sensitive synchrotron X-ray studies to provide a detailed description of SeCN^- adsorption at a floating charged monolayer. Polarimetry studies show that the average orientation of SeCN^- anions with respect to the surface normal decreases from 45° to 22° with the increasing KSeCN concentration. Interfacial SeCN^- coverage saturates at very low bulk concentrations, but their orientational organization, distribution between Stern and diffuse layers, and effects on the hydrogen-bonding network of the interfacial water continue to change with increasing bulk KSeCN concentration. These results show that the increasing chemical potential may lead to further reorganization of the adsorbed ions, even though the total interfacial ion population does not change. The reorganization of the interfacial ions and the water may be very important in chemical separations of heavy metals, where metal–anion complexes drive the selective ion transfer at aqueous interfaces.



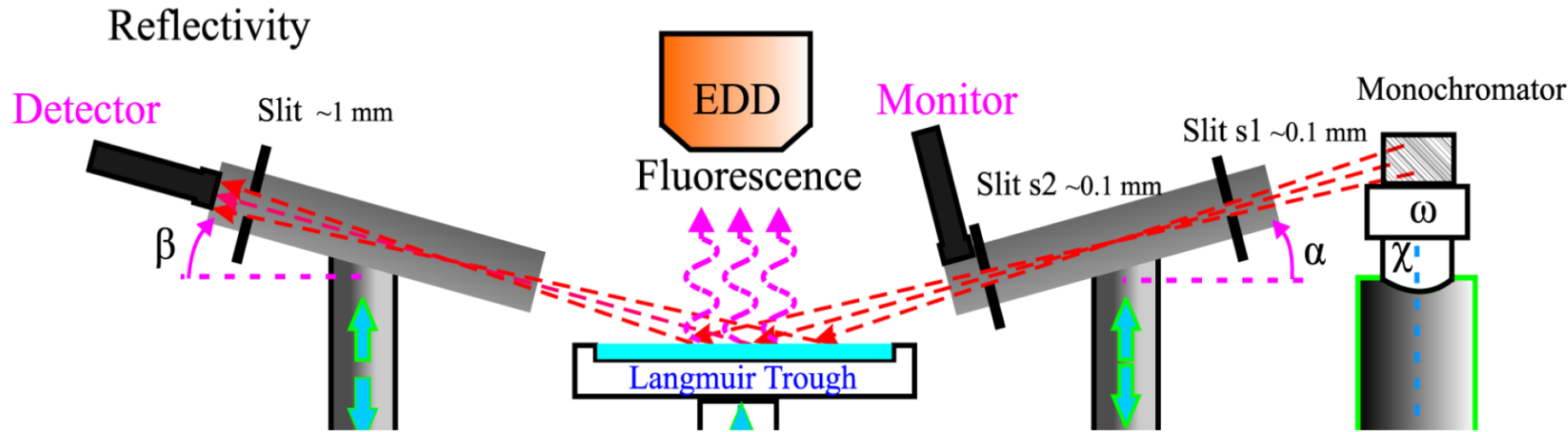
❖ Main idea

- ❖ Orientation of Selenocyanate (SeCN^-) change after increasing concentration at the the surface
- ❖ X-Ray proofs the population of SeCN^- at the interface at different concentration
- ❖ DPTAP- KSeCN not even decrease OH intensity but also show peak at 3700 cm^{-1} (free OH)

❑ Schematic set up



❑ X-ray fluorescence (XRF) and X-ray reflectivity (XRR) (Woongmo's thesis)



- ❑ X-ray energy 8.044 keV
- ❑ X-ray wavelength $\lambda = 1.542 \text{ \AA}$

- ❑ $Q_z = 4\pi \sin \alpha / \lambda$: wave vector,
- ❑ α : incident angle

❑ Below the critical angle, fluorescence intensity is

$$I_F(Q_z) = C |t(Q_z)|^2 n_s \exp[-|z_{\text{ion}}|/D(Q_z)] \quad (1)$$

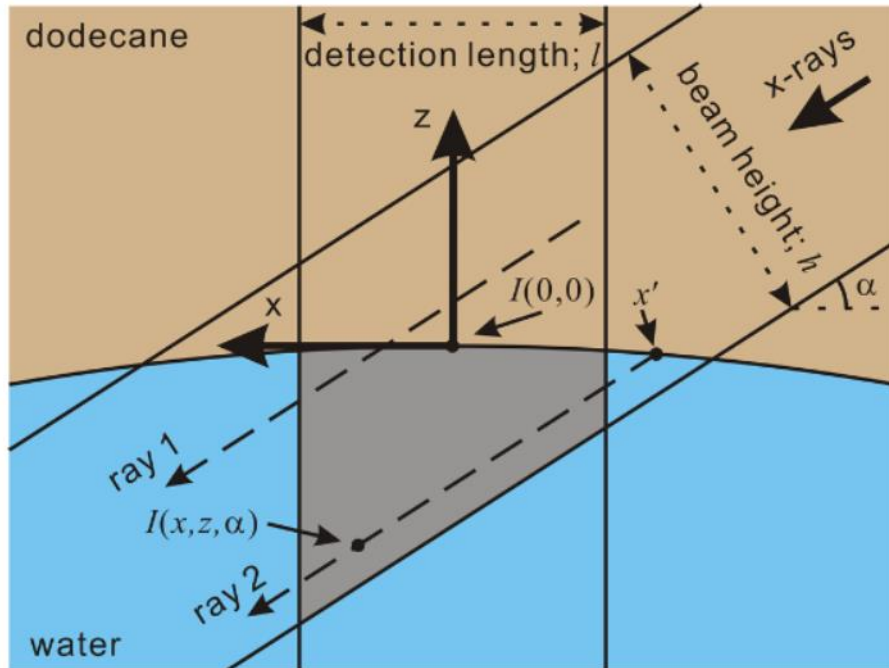
where C is a scale factor. $t(Q_z)$ and $D(Q_z)$ are calculated Fresnel amplitude transmission coefficient at the ideally flat and sharp air/water interface³² and X-ray penetration depth normal to the surface.³³ When α is larger than α_c , fluorescence intensity

❑ Above the critical angle, fluorescence intensity is

$$I_F(Q_z) = C |t(Q_z)|^2 D(Q_z) n_b \quad (2)$$

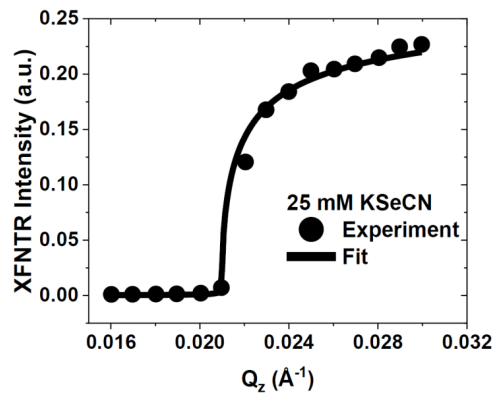
❑ X-ray fluorescence near total reflection (XFNTR)

J. Phys. Chem. B 2014, 118, 12486–12500



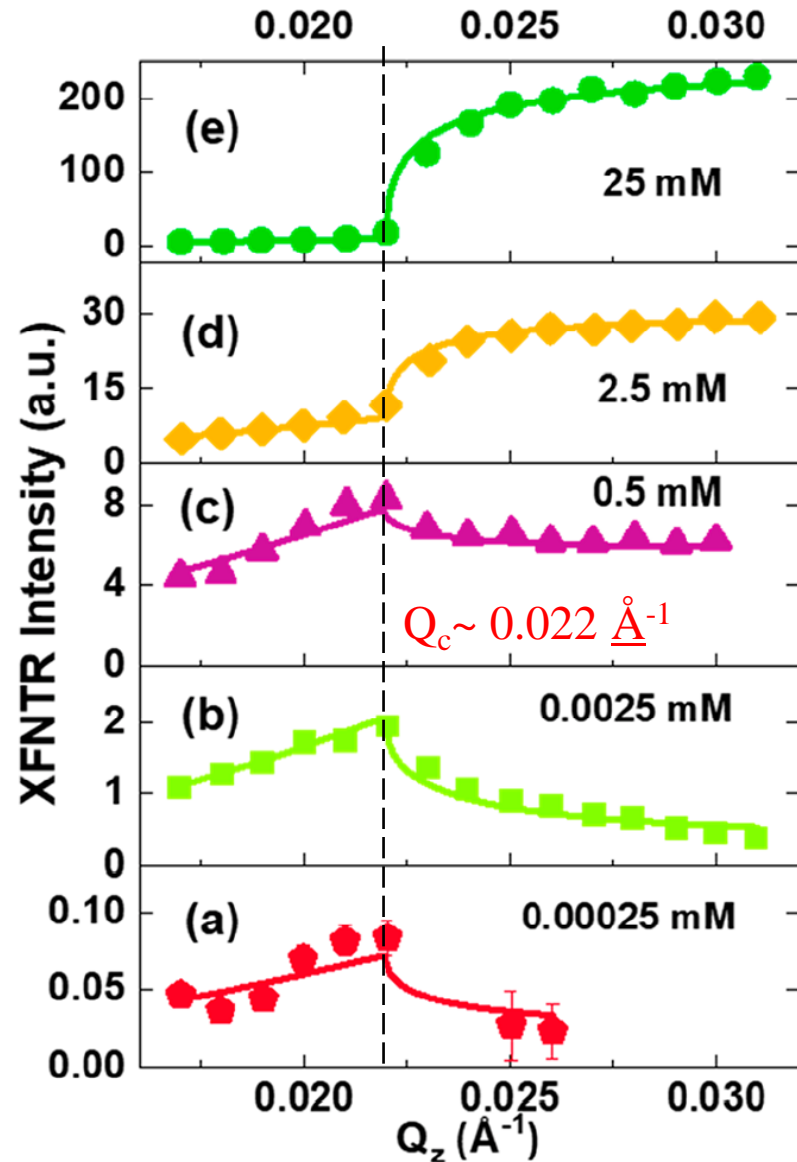
- ❑ X-ray energy 17.3 keV
- ❑ X-ray wavelength $\lambda = 0.73 \text{ \AA}$

$$\frac{I(x, z, \alpha_i)}{I(0,0)} = t_f(\alpha_i)^2 e^{-z/\Lambda} e^{-\mu_o x'}$$



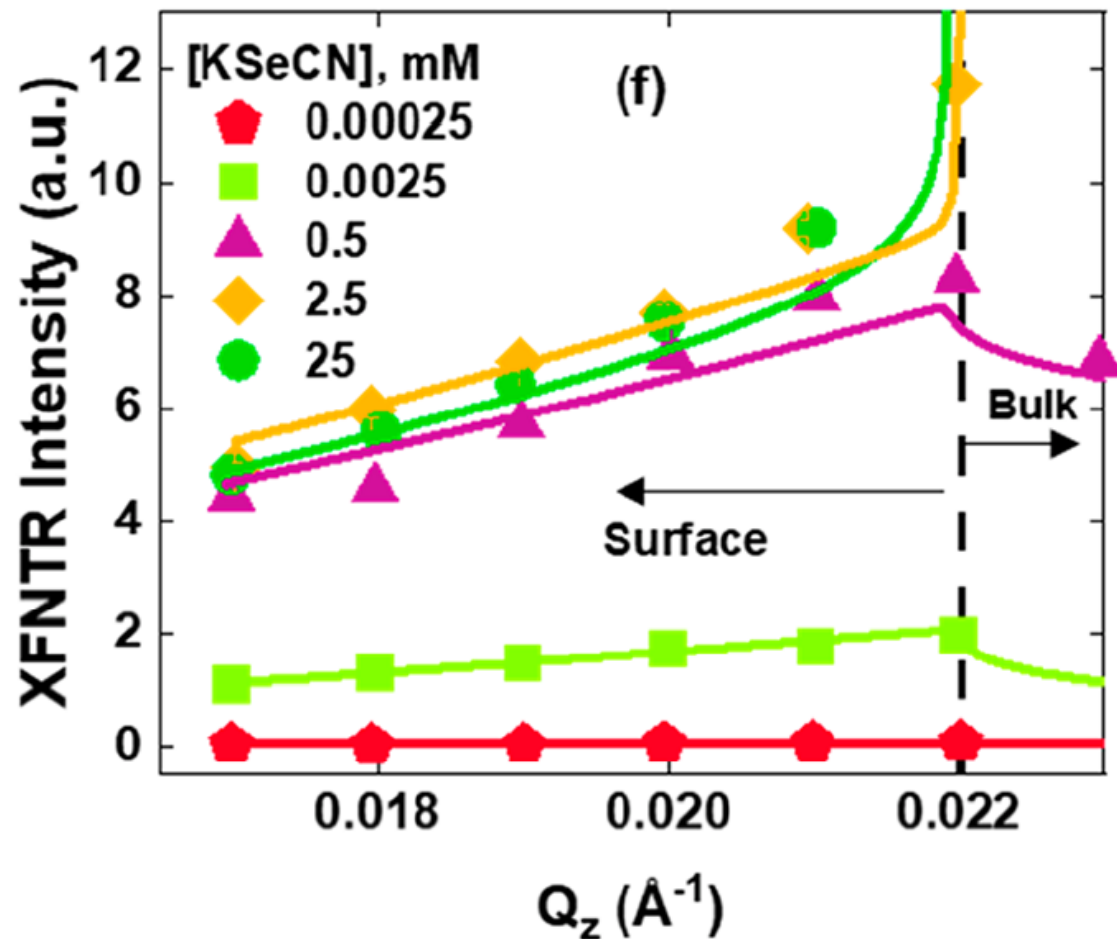
Where α_i , t_f , Λ , and μ_o refer to angle of incidence, Fresnel transmission factor, penetration depth, and the linear absorption coefficient of the top phase (Helium gas in our case). We do the following analysis by ignoring the $e^{-\mu_o x'}$ as X-ray absorption by He is small compared to other effects. The recorded fluorescence signal is then proportional to the integral of $\frac{I(z, \alpha_i)}{I(0,0)} \propto t_f(\alpha_i)^2 e^{-z/\Lambda}$ over the detection volume, after taking into account the density of the fluorescent species (Se atoms in our case). Variation of $I(\alpha_i, z)$ for a few angles above and below the critical

□ DPTAP-KSeCN by XFNTTR

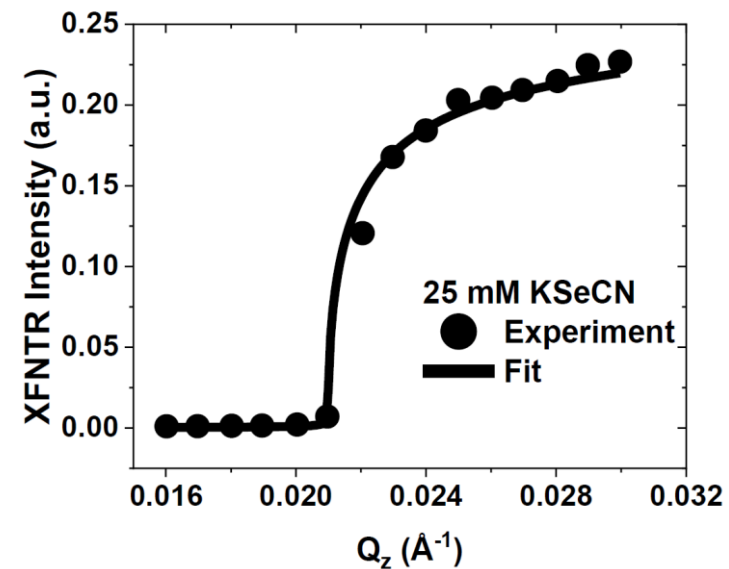


- ❖ Below critical angle ($Q_c \sim 0.022 \text{ \AA}^{-1}$) intensity increases linearly due to anion adsorption at the interface.
- ❖ $[\text{SeCN}^-] < 0.5 \text{ mM}$, intensity decreases (above Q_c) due to decreasing transmission and very small bulk concentration.
- ❖ $[\text{SeCN}^-] = 0.5 \text{ mM}$, number of SeCN^- anions is saturated due to neutrality between positively charged DPTAP and negatively anions
- ❖ Above Q_c does not mention the increasing after 0.5 mM !!

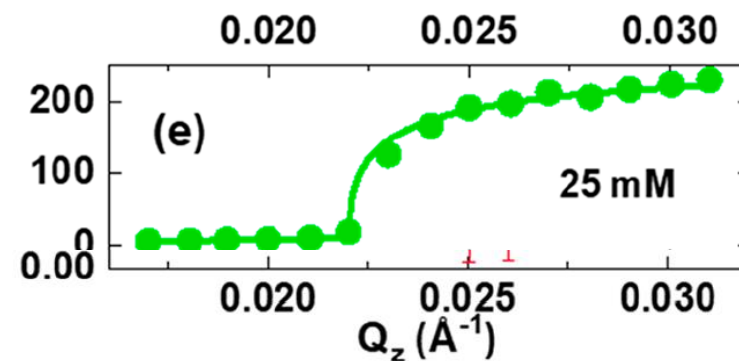
□ Summary of XFNTR results



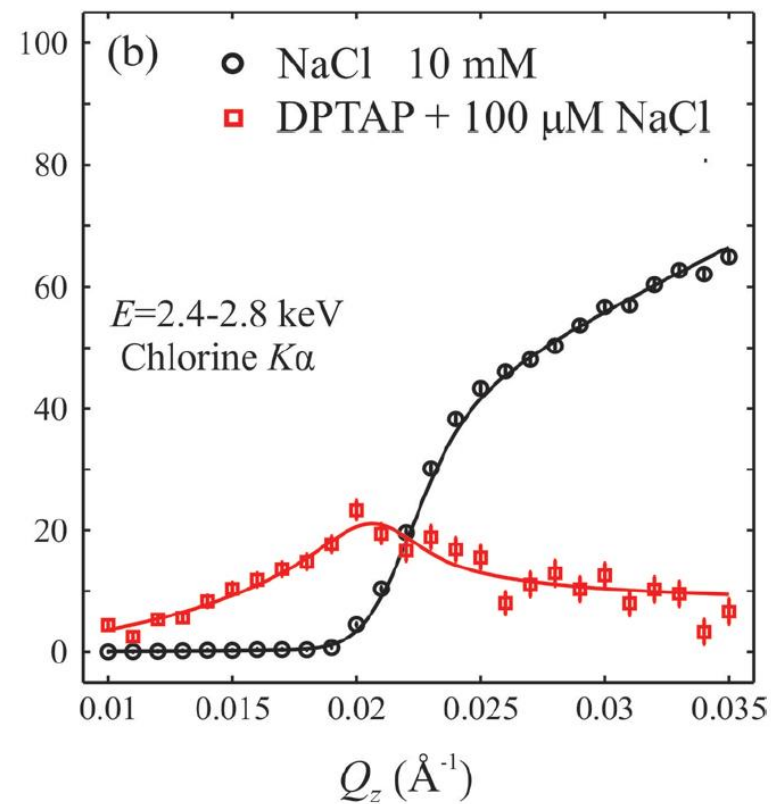
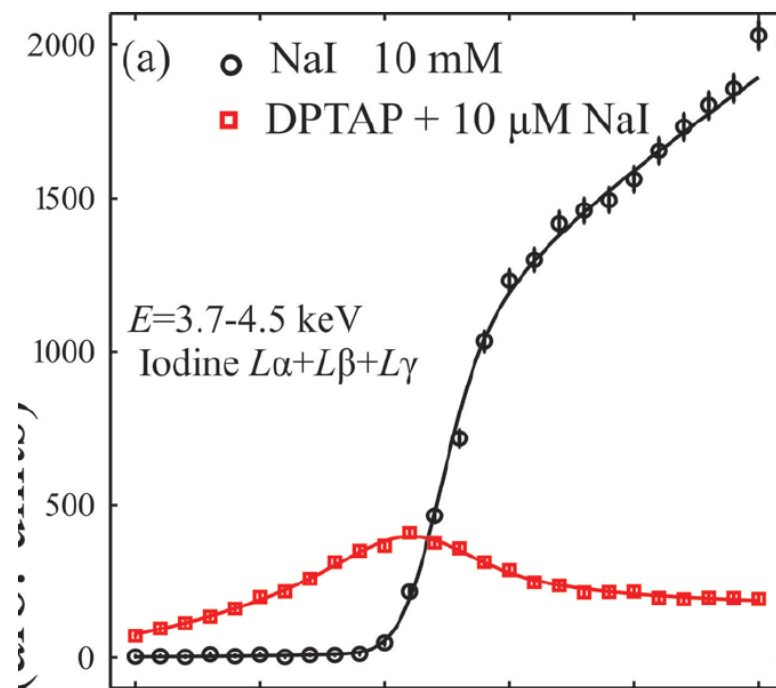
25 mM KSeCN without DPTAP



25 mM KSeCN with DPTAP

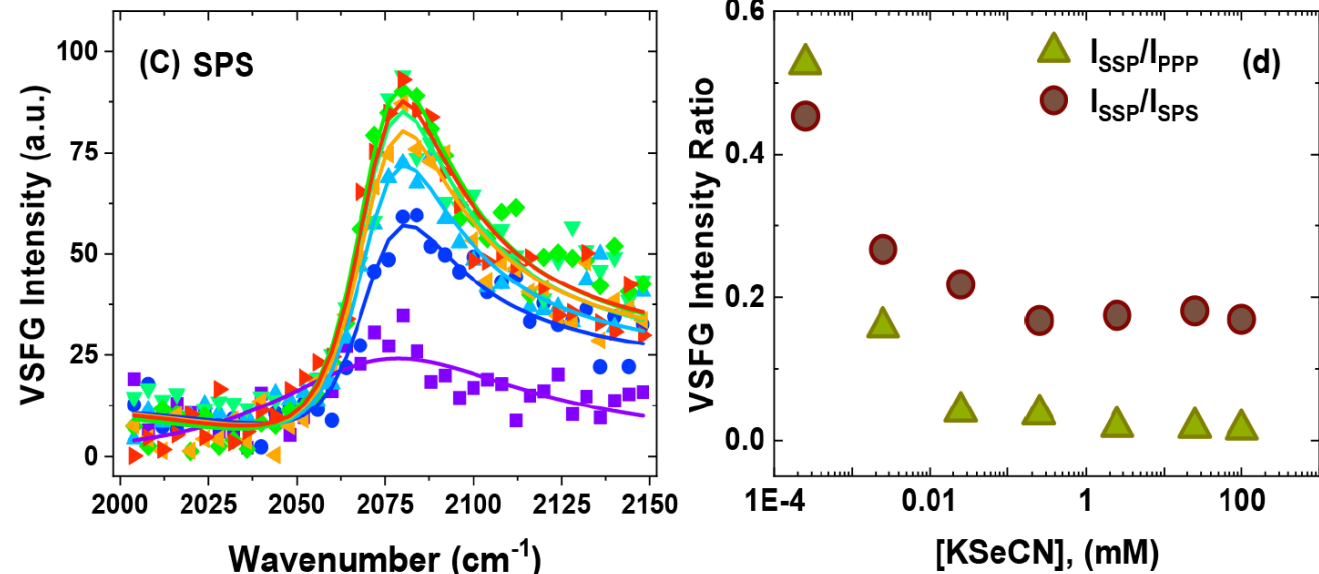
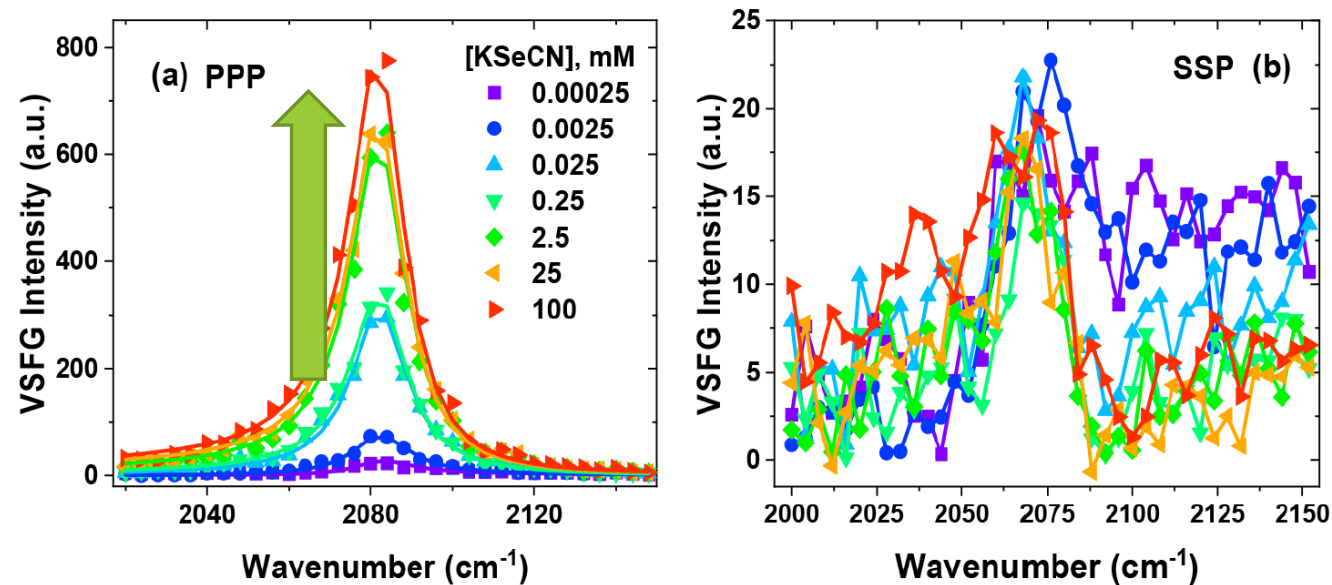


□ Comparing with woongmo's data

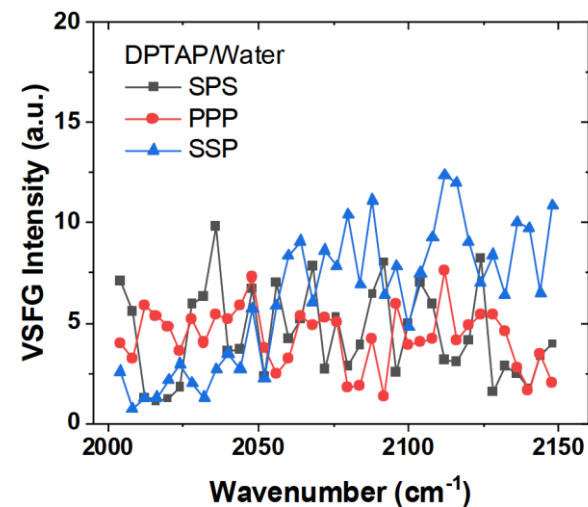


J. Phys. Chem. C 2015, 119, 7130–7137

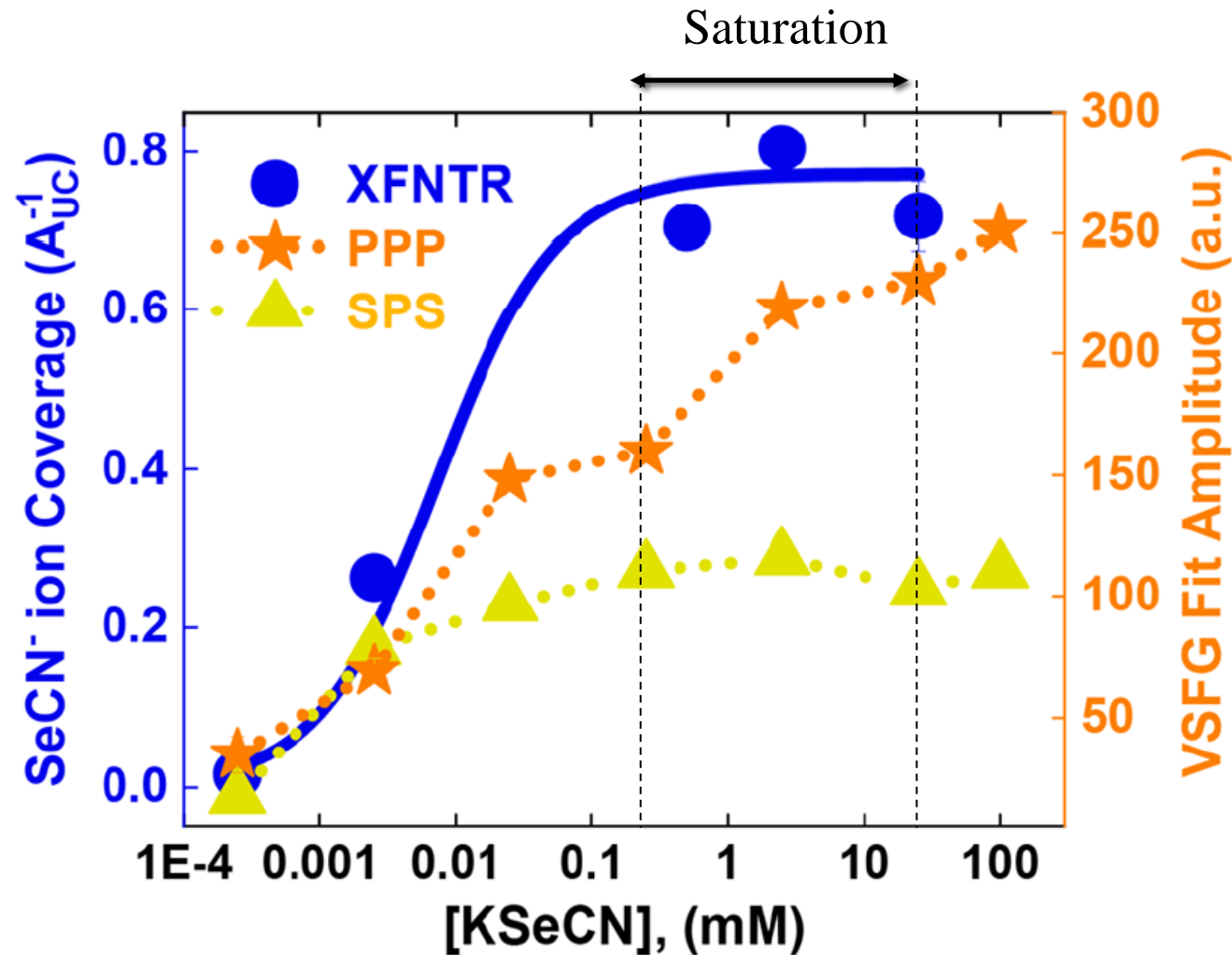
□ DPTAP-KSeCN by SFG at different polarizations



- ❖ Under **PPP** polarization, intensity of **SeCN⁻** is **monotonically increases** with increasing KSeCN concentration but not SSP, and SPS is slightly increased.
- ❖ Constructive interference between $\chi^{(2)}$ components and SeCN⁻
- ❖ By taking the ratio between I_{ssp}/I_{ppp} and I_{ssp}/I_{sps} determined the average orientation of anions from **45°** to **22°**

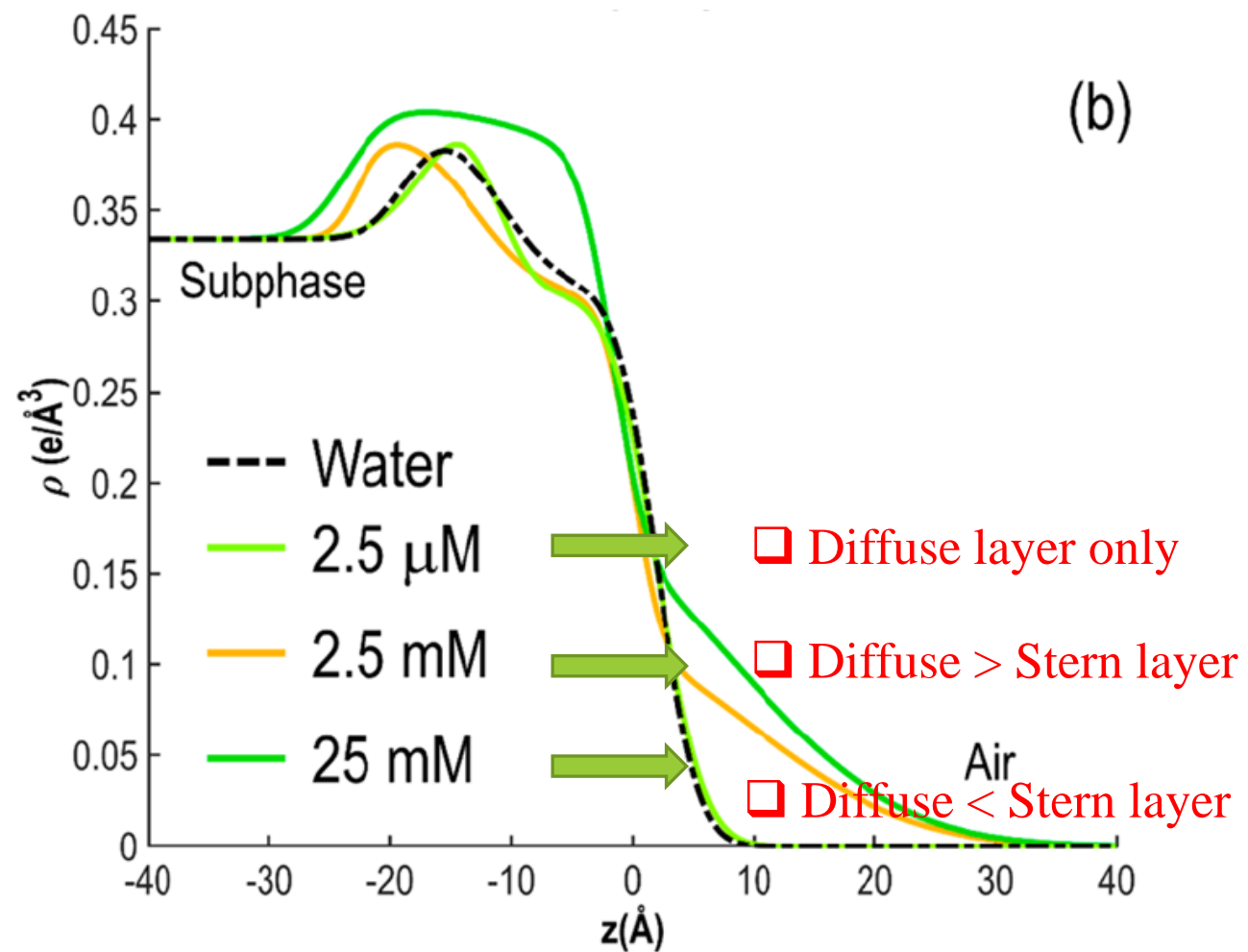
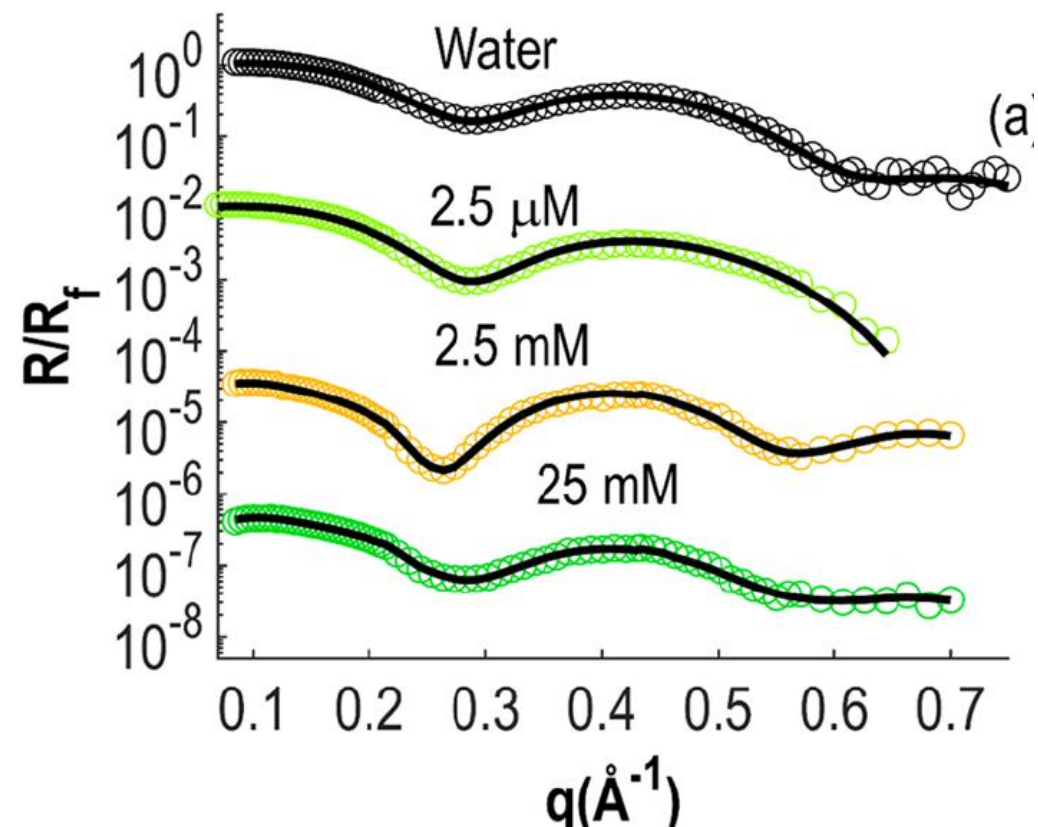


□ DPTAP-KSeCN by SFG at different polarizations

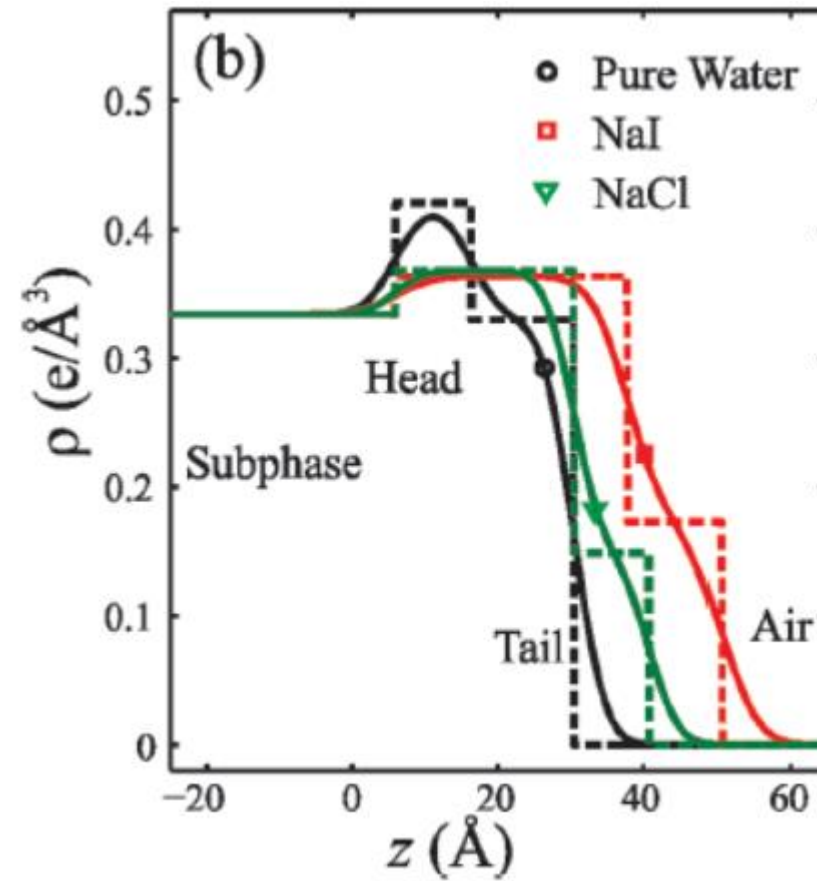
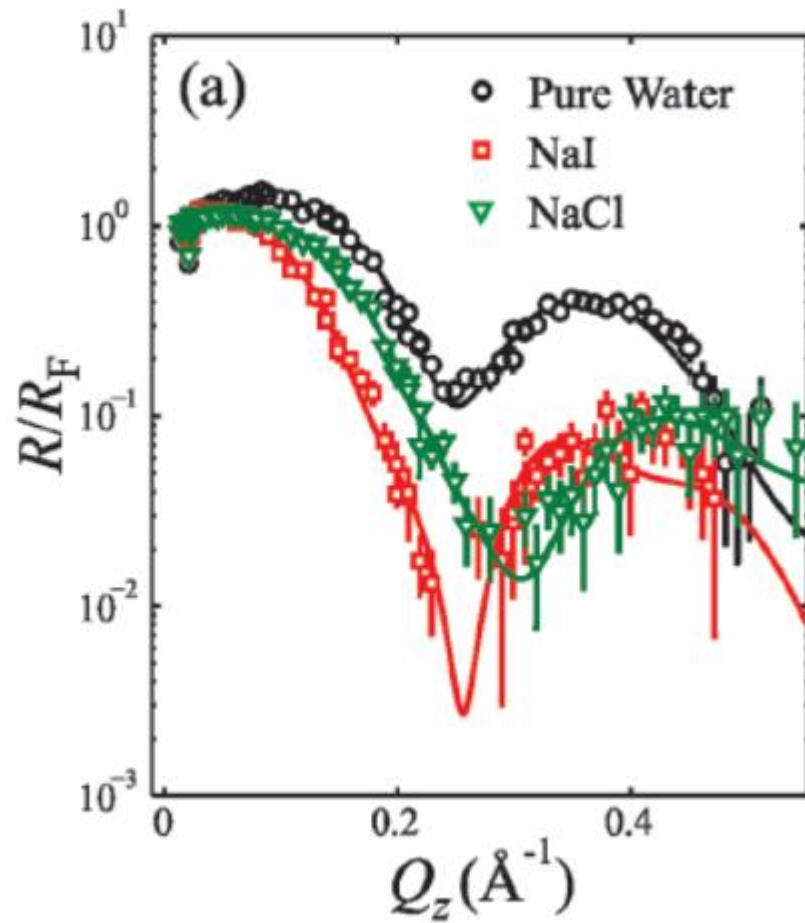


- From **XFNR** A_{UC} unit cell area of DPTAP and $1A_{UC}^{-1}$ mean 1 SeCN⁻:1 DPTAP molecule
- From **XFNR** and **SFG** under **SPS** polarization showing the saturation from **0.5 mM** indicated SeCN⁻ ions are saturated in both Stern and Diffuse layer
- But from SFG under PPP polarization does not show saturation.

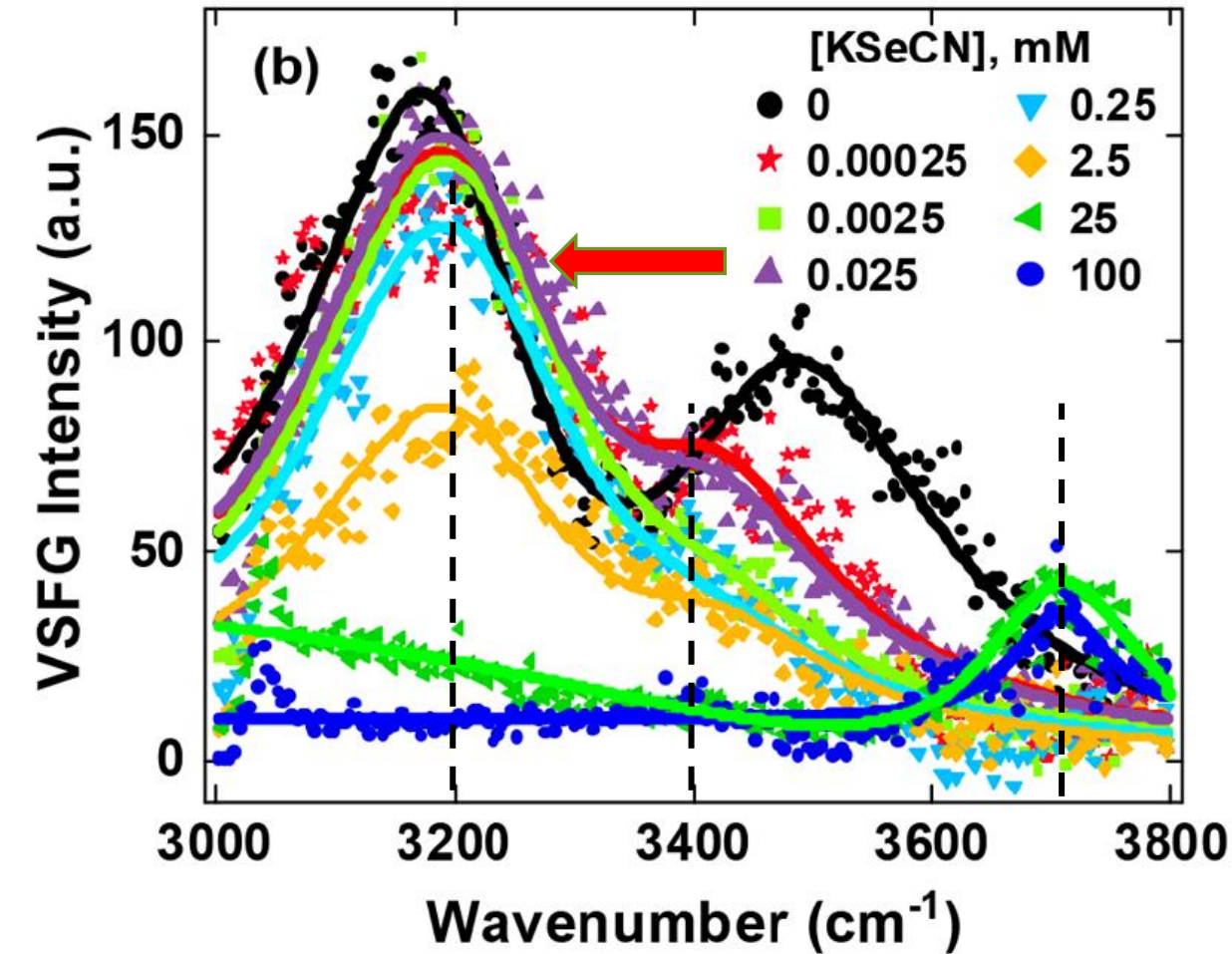
□ X-ray reflectivity intensity (R) normalize to Fresnel reflectivity (R_f) for an ideally flat interface



□ Comparing with woongmo's data



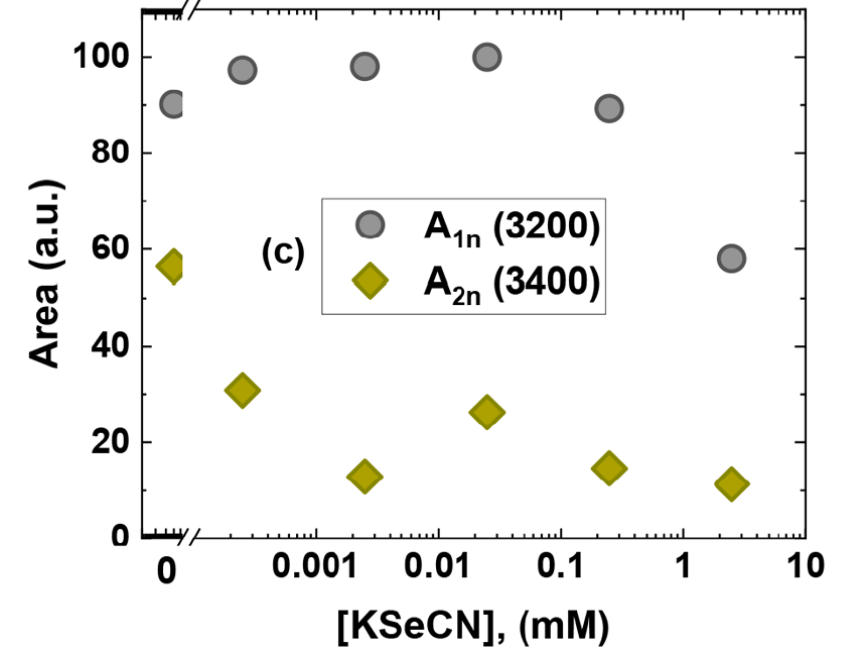
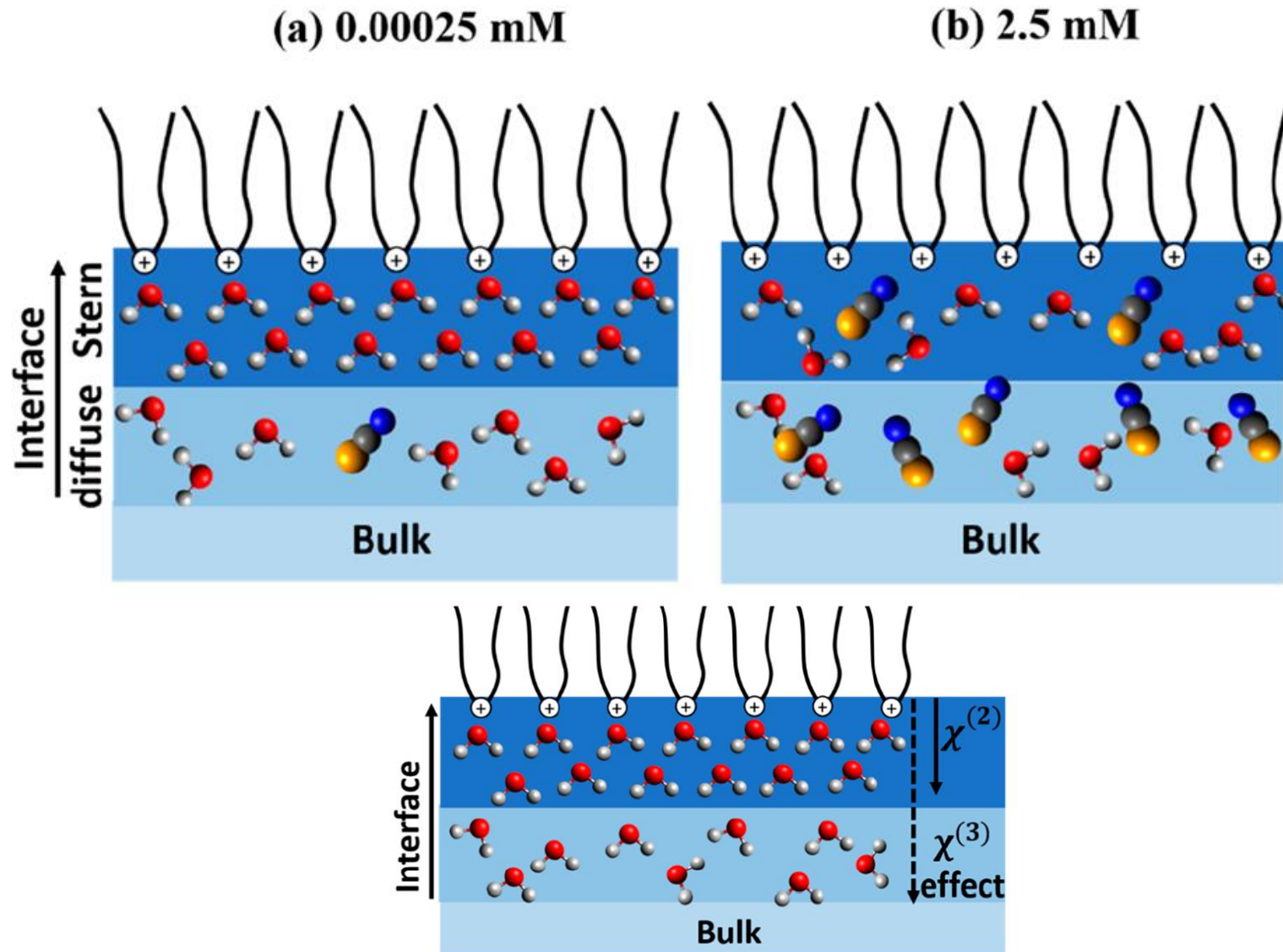
□ DPTAP-KSeCN at OH regions



- 3200 cm^{-1} strongly hydrogen-bonded OH
- 3400 cm^{-1} weakly hydrogen-bonded OH

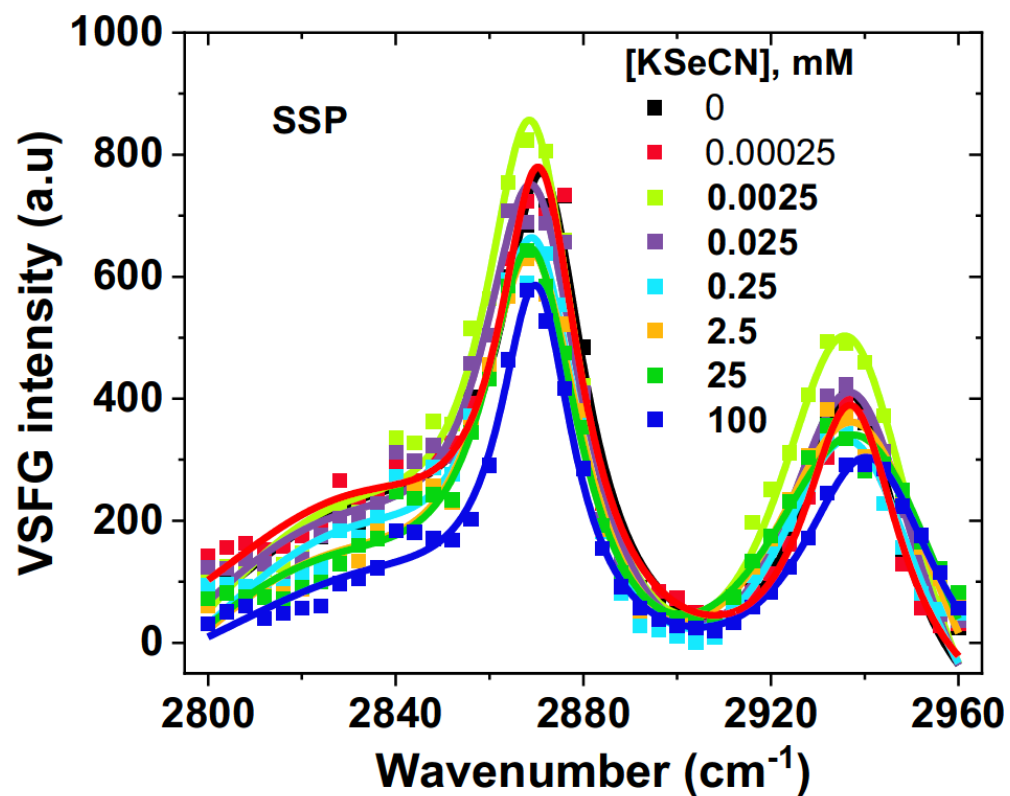
- OH intensities decreased due to charge screening effect
- 3400 cm^{-1} band is red shift after increasing salt concentration due to ions interacted with water surrounding. (in diffuse layer) (how's about 0.0025 mM ?)
- 3200 cm^{-1} band is affected at the concentration 0.25 mM and mostly from Stern layer
- At $\geq 25\text{ mM}$ both OH bands are disappeared and appeared of 3700 cm^{-1} peak

□ Anions moved from diffuse to stern layer after increasing concentration

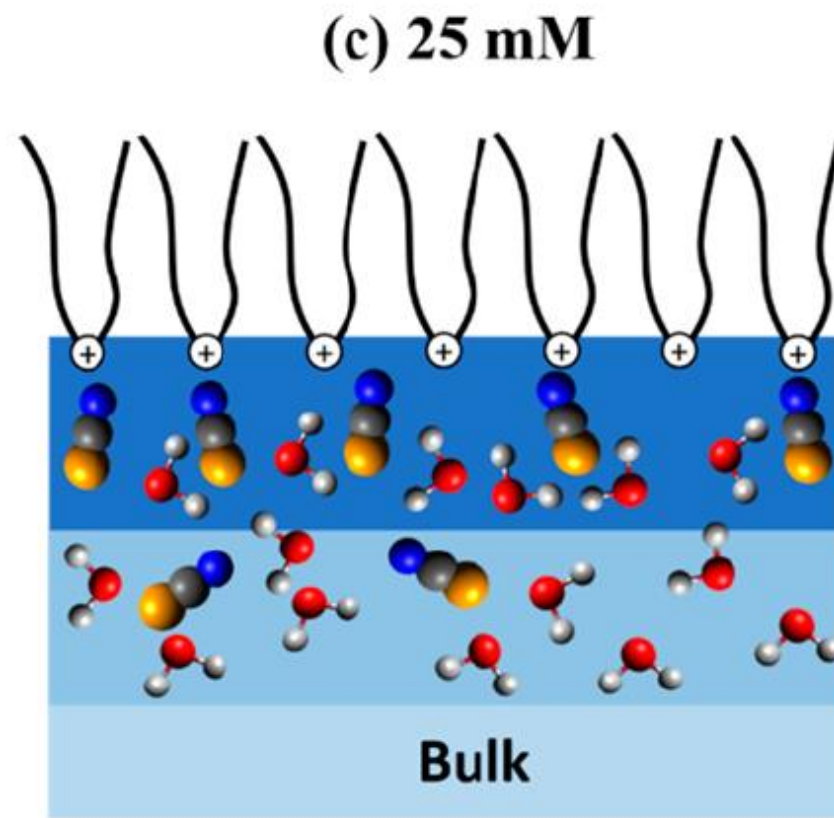


❑ Discussion of the appearance of 3700 cm^{-1} band (2 possible reasons)

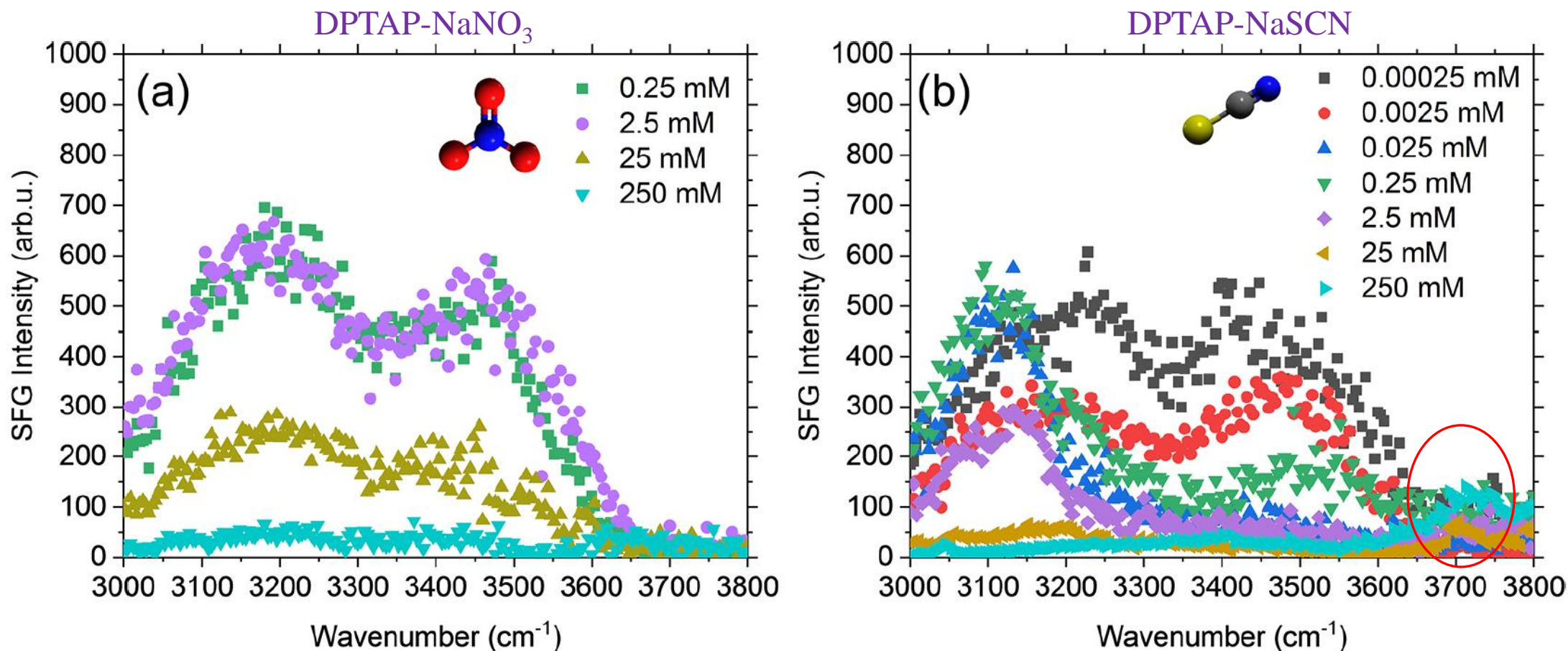
❖ Monolayer is disturbed and make a space for free OH but that is ruled out by the data below.



❖ Complex binding between $\text{SeCN}^-:\text{H}_2\text{O}$ as the increasing of anions at the stern layer



Previous study DPTAP- NaNO_3 / NaSCN



Finally, as the signal intensity from the bonded OH region decreases, a free OH peak appears, indicating disruption in the monolayer surface coverage. The shift and narrowing of the

Previous study DPTAP- PdCl_4^{2-} / PtCl_6^{2-}

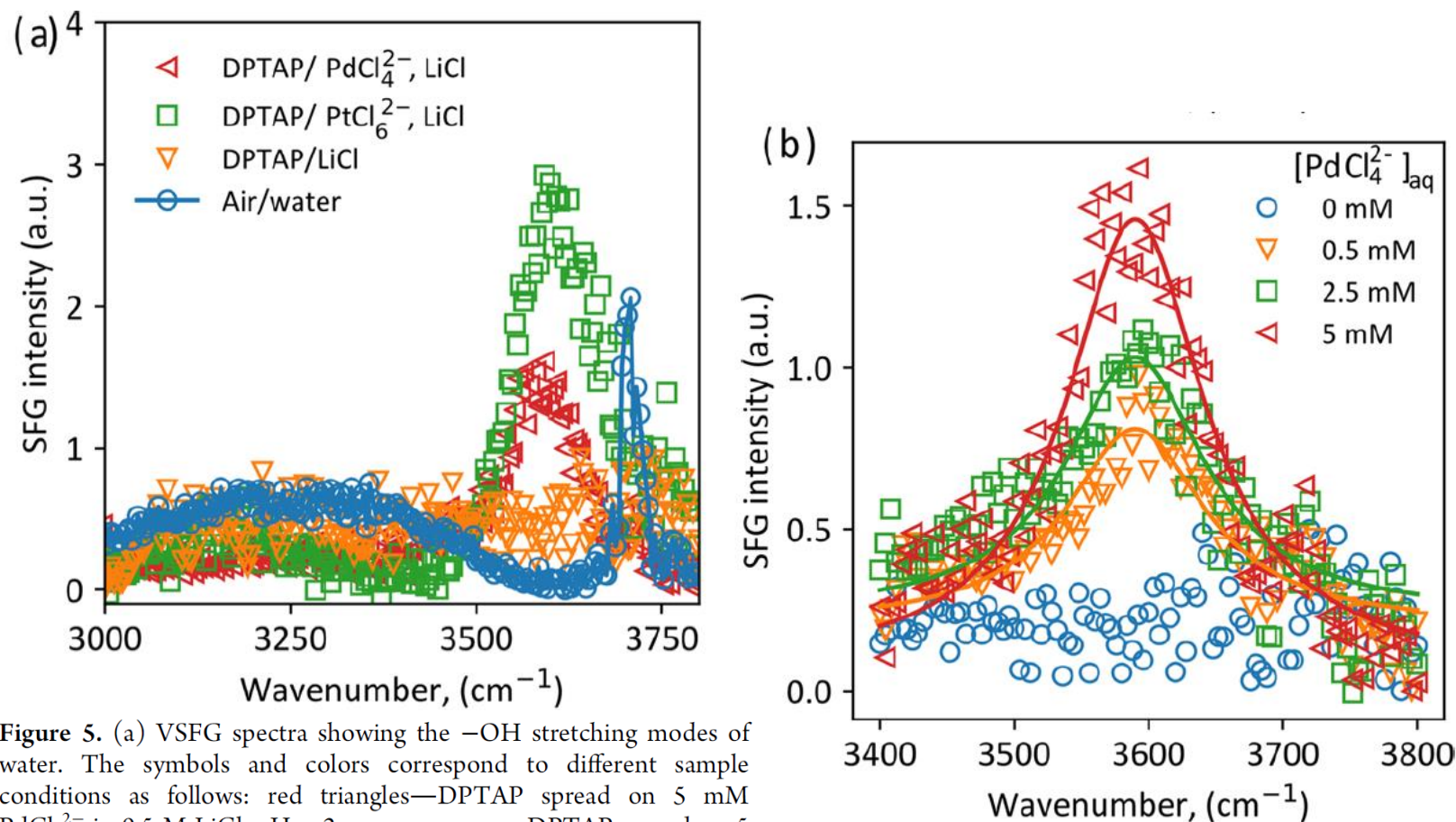
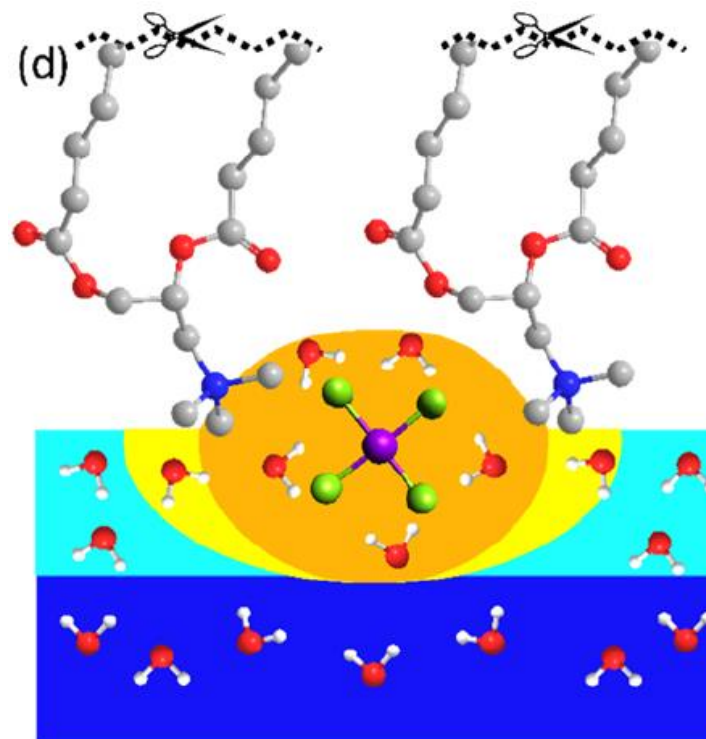
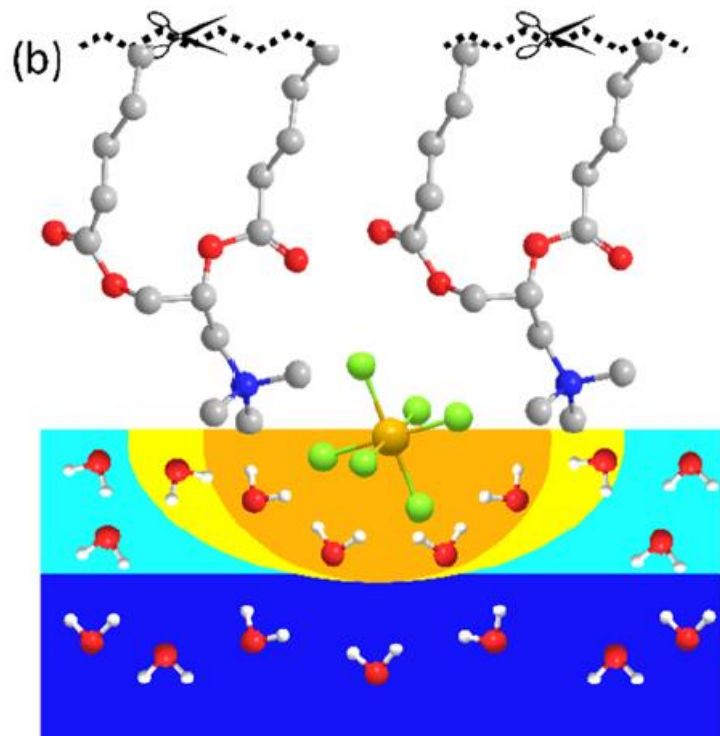


Figure 5. (a) VSFG spectra showing the $-\text{OH}$ stretching modes of water. The symbols and colors correspond to different sample conditions as follows: red triangles—DPTAP spread on 5 mM PdCl_4^{2-} in 0.5 M LiCl, pH = 2; green squares—DPTAP spread on 5 mM PtCl_6^{2-} in 0.5 M LiCl, pH = 2; orange inverted triangles—DPTAP spread on 0.5 M LiCl, pH = 2; and blue circles—air/water interface. (b) VSFG spectra showing the variation of the AIWHB peak with the concentration of PdCl_4^{2-} in the subphase. Symbols represent experimental data, whereas solid lines are fits to the experimental data obtained with eq 6. All samples contain 0.5 M LiCl and are kept at pH = 2.

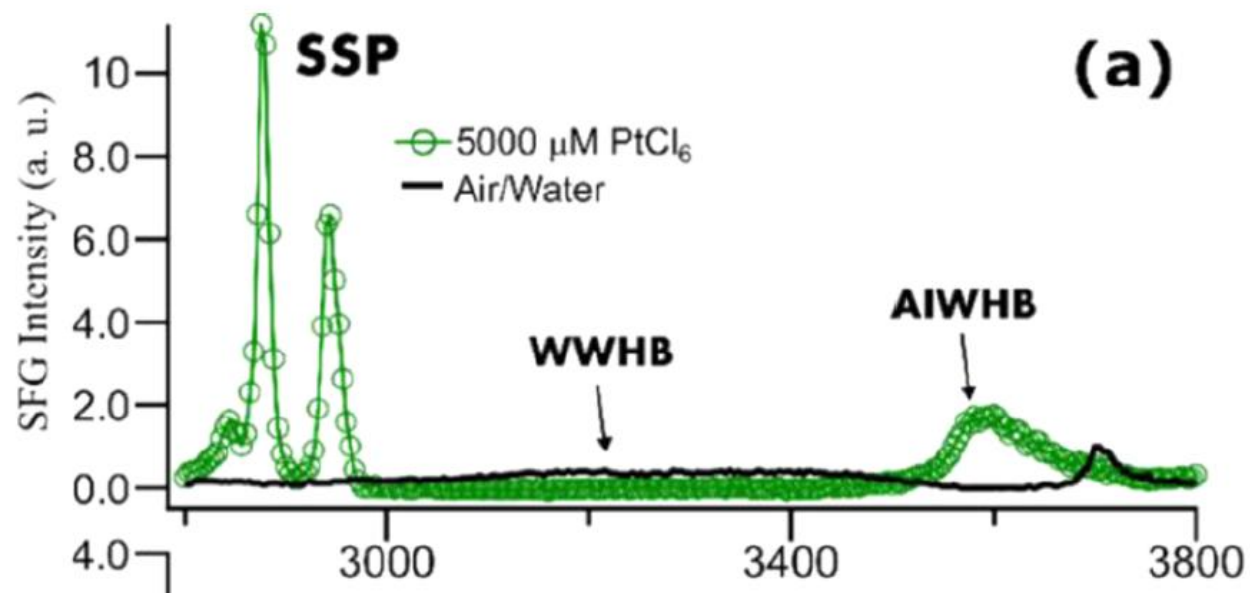
❖ The peak at $\sim 3600 \text{ cm}^{-1}$ is named as the anion-induced weak hydrogen-bonded (AIWHB).



■ WWHB-Up ■ AIWHB-Up
■ WWHB-Down ■ AIWHB-Down

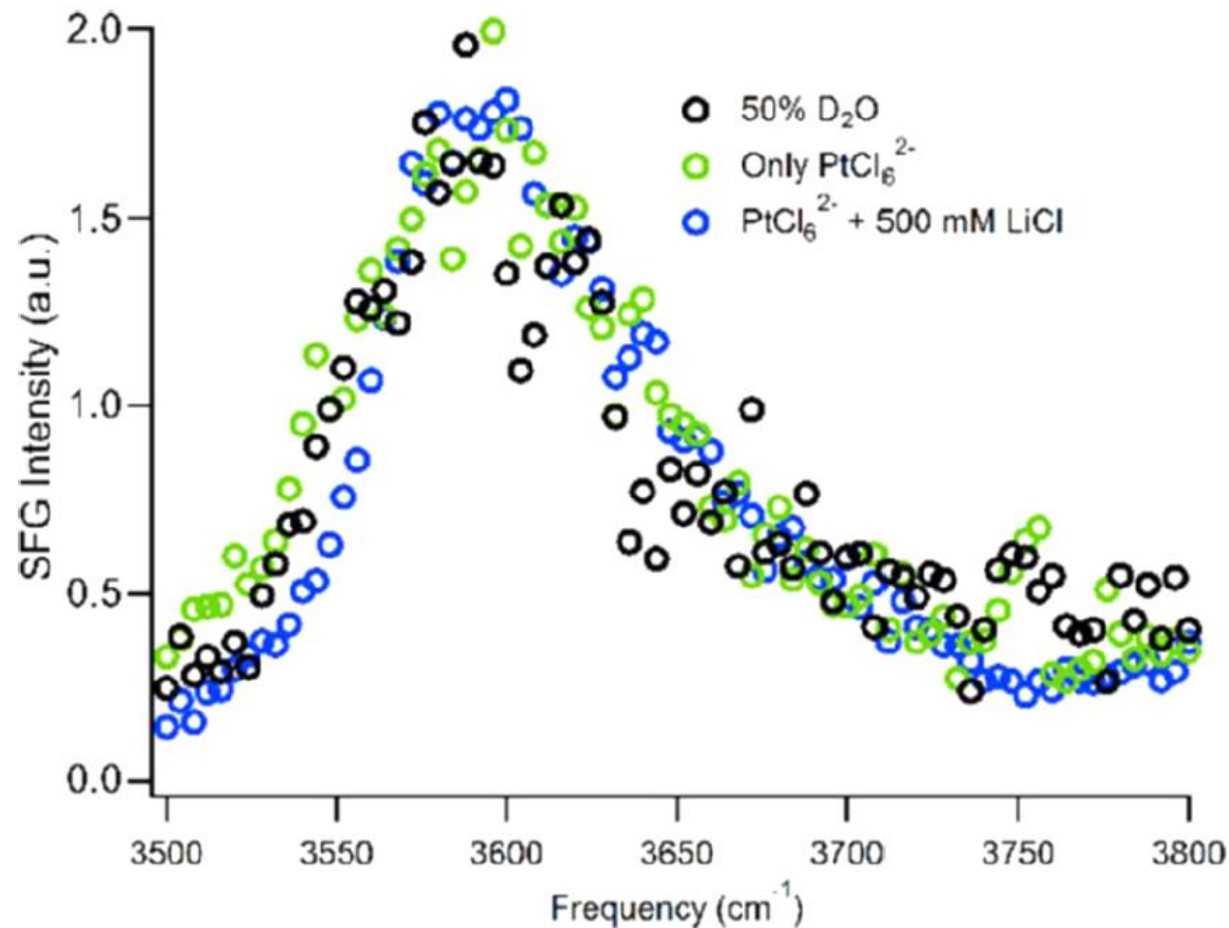
□ First finding AIWHB peak

DPTAP-PtCl₆



J. Phys. Chem. C 2018, 122, 29228–29236

DPTAP-PtCl₆ in H₂O = 2 DPTAP-PtCl₆
in 50:50 vol% of H₂O: D₂O



❑ In summary

Position of anions

❖ Diffuse layer

❖ Diffuse layer > Stern layer

❖ Diffuse layer < Stern layer
and appearance of 3700 cm^{-1} band

(a) 0.00025 mM

(b) 2.5 mM

(c) 25 mM

